Ultra-broadband wavelength-swept Tm-doped fiber laser using wavelength-combined gain stages

M. Tokurakawa, [1,3,*] J. M. O. Daniel,[1,4] C. S. Chenug,[2] H. Liang,[2] and W. A. Clarkson[1]

1. Optoelectronics Research Centre, University of Southampton, Highfield, SO17 1BJ, UK
2. School of Science & Technology, Nottingham Trent University, Nottingham NG11 8NS, UK
3. Present address: Institute of Laser Science, University for Electro-Communications, 1-5-1 Cho-fugaoka, Cho-fu, 182-8585, Tokyo, Japan
4. Present address: Aether Photonics, Melbourne Australia
**tokura@ils.uec.ac.jp*

Abstract: A wavelength-swept thulium-doped fiber laser system employing two parallel cavities with two different fiber gain stages is reported. The fiber gain stages were tailored to provide emission in complementary bands with external wavelength-dependent feedback cavities sharing a common rotating polygon mirror for wavelength scanning. The wavelength-swept laser outputs from the fiber gain elements were spectrally combined by means of a dichroic mirror and yielded over 500 mW of output with a scanning range from ~1740 nm to ~2070 nm for a scanning frequency of ~340 Hz.

OCIS codes: (140.3510) Lasers, fiber; (140.3600) Lasers, tunable; (060.3510) Lasers, fiber.

References and links

1. W. A. Clarkson, A. Abdolvand, D. Y. Shen, R. A. Hayward, L. J. Cooper, R. B. Williams, and J. Nilsson, "High power two-micron fibre lasers," Proc. SPIE **5120**, 482–489 (2003).
2. P. F. Moulton, G. A. Rines, E. V. Slobodtchikov, K. F. Wall, G. Frith, B. Samson, and A. L. G. Carter, "Tm-Doped Fiber Lasers: Fundamentals and Power Scaling," IEEE J. Sel. Top. Quantum Electron. **15**(1), 85–92 (2009).
3. T. Ehrenreich, R. Leveille, I. Majid, K. Tankala, G. Rines, and P. Moulton, "1-kW, all-glass Tm:fiber laser," Proc. SPIE **7580**, 112 (2010).
4. S. D. Agger and J. H. Povlsen, "Emission and absorption cross section of thulium doped silica fibers," Opt. Express **14**(1), 50–57 (2006).
5. S. R. Chinn, E. A. Swanson, and J. G. Fujimoto, "Optical coherence tomography using a frequency-tunable optical source," Opt. Lett. **22**(5), 340–342 (1997).
6. H. Liang, R. Lange, B. Peric, and M. Spring, "Optimum spectral window for imaging of art with optical coherence tomography," Appl. Phys. B **111**(4), 589–602 (2013).
7. J. Geng, Q. Wang, J. Wang, S. Jiang, and K. Hsu, "All-fiber wavelength-swept laser near 2 μm," Opt. Lett. **36**(19), 3771–3773 (2011).
8. M. Tokurakawa, J. M. O. Daniel, C. S. Chenug, H. Liang, and W. A. Clarkson, "Wavelength-swept Tm-doped fiber laser operating in the two-micron wavelength band," Opt. Express **22**(17), 20014–20019 (2014).
9. D. Y. Shen, J. K. Sahu, and W. A. Clarkson, "High-power widely tunable Tm:fibre lasers pumped by an Er,Yb co-doped fibre laser at 1.6 mum," Opt. Express **14**(13), 6084–6090 (2006).
10. W. Y. Oh, S. H. Yun, G. J. Tearney, and B. E. Bouma, "Wide Tuning Range Wavelength-Swept Laser With Two Semiconductor Optical Amplifiers," IEEE Photon. Technol. Lett. **17**(3), 678–680 (2005).
11. S. H. Yun, C. Boudoux, G. J. Tearney, and B. E. Bouma, "High-speed wavelength-swept semiconductor laser with a polygon-scanner-based wavelength filter," Opt. Lett. **28**(20), 1981–1983 (2003).

1. Introduction

Over the last decade, two-micron fiber lasers have attracted considerable attention owing to a wealth of applications. Compared with Yb-doped fiber lasers operating in the one-micron band, they offer the advantage of a much higher maximum permissible eye exposure limit aiding deployment in demanding environments for industrial, defense, ranging and free-space communication applications. Moreover, the potential to use larger core areas whilst maintaining single-mode operation offers the prospect of higher powers before the onset of

#226592 - $15.00 USD Received 10 Nov 2014; revised 19 Dec 2014; accepted 20 Dec 2014; published 8 Jan 2015

damage or detrimental nonlinear loss processes, such as stimulated Brillouin scattering and Raman scattering [1, 2]. Tm-doped glass fiber is one of the most attractive gain media for 2 μm laser operation. Owing to a fortuitous two-for-one cross-relaxation process ($^3H_4 + {}^3H_6 \Rightarrow {}^3F_4 + {}^3F_4$) in combination with an appropriately tailored fiber design, laser diode (LD) pumping can be highly efficient. Moreover, the fiber geometry allows relatively simple thermal management and provides a high degree of immunity from the deleterious effects of thermal loading. These features have allowed power scaling of cladding-pumped Tm-doped fiber lasers to the kW regime [3]. Tm-doped silica glass also benefits from a very broad emission spectrum spanning the wavelength range from ~1700 nm to ~2100 nm [4] allowing wide flexibility in operating wavelength, which, in turn opens up the prospect of wavelength-swept laser sources with a very broad tuning range. From an applications perspective, wavelength-swept lasers (WS-lasers) operating in the two-micron band are particularly interesting. Rapid 'real-time' spectroscopic characterization of materials and swept-source optical coherence tomography (SS-OCT) [5] are two important examples of such applications. The use of OCT for non-invasive investigation of paintings to provide the information necessary for effective restoration and to aid conservation, art history and archaeology is one emerging application where operation in the longer wavelength band around ~2 μm brings the advantage of increased penetration depth due to reduced scattering for typical artists' pigments [6]. Tm-doped silica fiber laser provide an efficient way to access the relevant wavelength region due to the wide emission band for Tm-doped silica glass. Recently, wavelength-swept Tm-doped fiber lasers based on the use of a fiber Fabry-Perot Tunable Filter [7] and a feedback cavity containing a diffraction grating and rotating slotted-disk [8] were reported. Both configurations employed a single Tm fiber gain element and had scanning ranges of 200 nm or less. Wavelength tuning across the entire emission band (~1700 nm to ~2100 nm) with a single fiber gain stage is extremely difficult due to the combination of varying quasi-three-level character as a function of wavelength and gain saturation caused by short wavelength amplified spontaneous emission [9]. In order to access the full emission bandwidth potential of Tm-doped fiber laser, a different approach must be employed with two or more fiber gain stages and with each gain stage tailored to provide emission in complementary bands.

In this paper, we describe a wavelength-swept Tm-doped fiber laser system employing two parallel cavities with two different fiber gain stages to achieve wide wavelength scanning. The two fiber gain stages were tailored to have emissions in complementary bands with external wavelength-dependent feedback cavities sharing a common rotating polygon mirror for wavelength scanning. The wavelength-swept laser outputs from the fiber gain elements were spectrally combined by means of a dichroic mirror and yielded over 500 mW of output with a scanning range of 330 nm from ~1740 nm to ~2070 nm for a scanning frequency of ~340 Hz. To the best of our knowledge, this is the widest wavelength sweeping range reported to date for a wavelength-swept Tm fiber laser or indeed any fiber laser.

2. Design for wavelength-combined wavelength-swept laser

The experimental set-up for the wavelength-swept Tm fiber laser (WS-laser) is illustrated in Fig. 1. The WS-laser system had two parallel laser cavities with different Tm fiber gain stages and a common rotating polygon mirror feedback element. The first cavity (see lower part of Fig. 1) employed a double-clad Tm silica fiber gain stage with an 11-μm diameter core (NA ≈0.15) and a 125-μm diameter D-shaped pure silica inner-cladding surrounded by a low refractive index polymer coating. The fiber length and Tm doping concentration were 3 m and ~2 wt%, respectively. The fiber was cladding-pumped by a 793-nm fiber-coupled LD, which was free-spaced coupled into the output end of the fiber via an arrangement of lenses and a dichroic mirror to separate the laser output from the pump beam. The second cavity (see upper part of Fig. 1) utilized a core-pumped Tm silica fiber with a 10-μm diameter core (NA

#226592 - $15.00 USD Received 10 Nov 2014; revised 19 Dec 2014; accepted 20 Dec 2014; published 8 Jan 2015

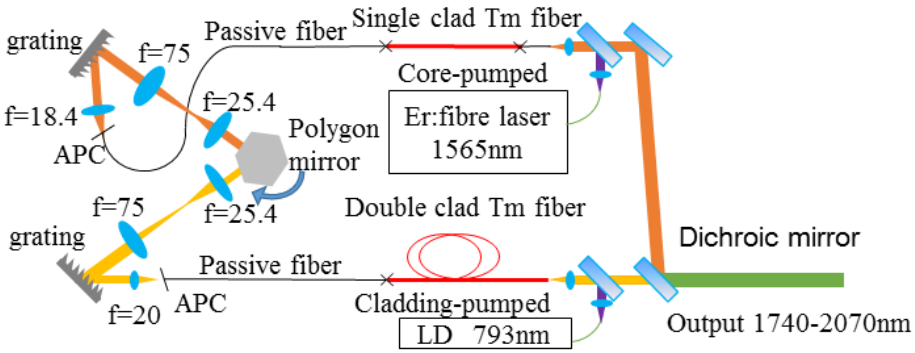

Fig. 1. Schematic diagram of the wavelength swept Tm-doped fiber laser with two gain stages. The upper part is the core-pumped configuration and the lower part is the cladding-pumped configuration. Cross marks in the Fig. are splicing points. APC is angled fiber facet.

≈0.13). The fiber length and Tm doping concentration were 0.9 m and ~0.2 wt%, respectively. Pump light was provided by a commercial Er,Yb fiber laser at 1565 nm that was launched into the core of a passive single-mode fiber spliced to the output end of the active fiber. The passive fiber was employed to mitigate thermally induced misalignment. Once again a free-space pump incoupling arrangement was employed with a dichroic mirror to separate laser output and pump paths. The use of a core-pumped fiber with a low Tm doping level and short length yields a much higher population inversion density than in a cladding-pumped fiber configuration and hence provides the necessary gain at the short wavelength end of the emission band to access lasing in this region. Thus, cladding and core-pumped fiber stages naturally provide gain and hence laser emission at the long and short wavelengths ends of the Tm emission spectrum. Fine tailoring of the wavelength positions of the gain maxima can be achieved via careful selection of the fiber lengths. In both cases, feedback for lasing was provided by the Fresnel reflection from a perpendicularly-cleaved facet at the output end of the fiber and at the other end by an external feedback cavity. A single mode passive fiber (spliced to the active fibers) with an angled fiber facet at the fiber end adjacent to the external cavity was used to suppress broadband feedback and hence parasitic lasing between the fiber ends. The external cavities comprised a collimating lens, a blazed grating with 600 lines/mm at the center wavelength of 1600 nm, a telescope and rotating polygon mirror as the final feedback element. The latter was common to both external cavities and had a diameter of 35 mm with 6 facets of 2 mm thickness. As the polygon mirror rotates the angle at which the feedback light is incident on the diffraction grating changes and hence the feedback wavelength also changes. The polygon mirror based wavelength scanning filter used in our WS-laser system is similar to that reported in Ref [10]. for a WS-laser based on semiconductor gain media. The use of a common polygon mirror with parallel laser cavities ensures that the WS-laser outputs from both core and cladding-pumped Tm-doped fiber lasers are passively synchronized. In the core-pumped laser configuration, one molded aspherical glass lens (f = 18.4 mm) and two fused silica spherical glass lenses (f = 25.4 mm and 75 mm) were employed for the collimating lens and in the telescope, respectively. In the cladding-pumped laser configuration, fused silica and CaF_2 spherical lenses (f = 20mm, 25.4 mm and 75 mm) were employed to reduce material absorption loss beyond ~2050 nm. The free-spectral-range (FSR), resolution and scanning bandwidth of the wavelength scanning filter depend on the focal lengths of the lenses, the clear aperture dimensions of the telescope lenses, the diffraction grating pitch and facet length of polygon mirror [11]. For the set-up shown in Fig. 1, the FSR, resolution and scanning bandwidth were to be ~510 nm, ~0.25 nm and ~280 nm, respectively. In the estimation, we assumed a clear aperture of 20 mm for the telescope lenses and ignored effect of lens aberrations. The output beams from the core and cladding-pumped WS-lasers were spectrally-combined with the aid of a dichroic mirror.

#226592 - $15.00 USD Received 10 Nov 2014; revised 19 Dec 2014; accepted 20 Dec 2014; published 8 Jan 2015

3. Results & discussion

Prior to operation in the WS-laser configuration, the core and cladding-pumped Tm fibers were tested in the simple tunable cavity configuration shown in Fig. 2(a). In both cases, wavelength-dependent feedback was achieved with the aid of an external feedback cavity arrangement containing a diffraction grating and terminated by a broadband high reflectivity plane mirror. Wavelength tuning was achieved by simply adjusting the angle of the plane mirror. The distance between the angled fiber facet (APC in Fig. 1(a)) and the collimating lens was optimized during the wavelength tuning experiments to compensate for chromatic aberration in the collimating lens in order to maximize feedback efficiency at any particular wavelength. The core-pumped laser configuration had a tuning range of 280 nm; from 1730 nm to 2010 nm. The maximum output power was 1.66 W at 1855 nm for a launched pump power of ~3.9 W at 1565 nm. The cladding-pumped laser configuration had a tuning range of 200 nm; from 1900 nm to 2100 nm. The maximum output power was 0.75 W at 1990 nm for a launched pump power of 5.4 W at 793 nm. Thus, both lasers could be tuned over complementary bands and the total (combined) tuning range was 370 nm; from 1730 nm to 2100 nm [Fig. 2(b)].

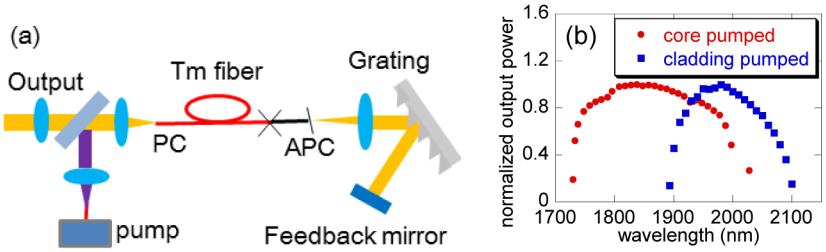

Fig. 2. (a) Schematic diagram of the manually tunable Tm laser configuration. (b) Wavelength tuning curves for cladding-pumped and core-pumped Tm fiber lasers.

WS-laser operation of each cavity incorporating the rotating polygon wavelength scanning filter (Fig. 1) was then investigated. In each case the alignment of the external cavity was optimized to achieve a broad and uniform output spectrum. The measured spectra of core and cladding-pumped WS-laser are show in Figs. 3(a) and 3(b) (optical spectrum analyzer,

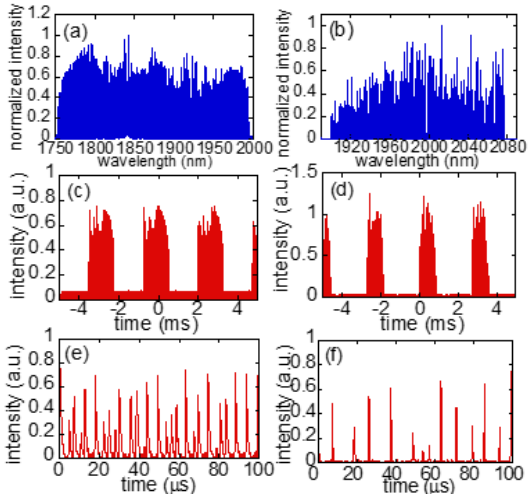

Fig. 3. (a) Output spectrum of core-pumped WS-laser. (b) Output spectrum of cladding-pumped WS-laser. (c) and (d) Temporal characteristics of the core and cladding-pumped WS lasers, respectively. (e) and (f) Expanded temporal characteristics of the core and cladding-pumped WS lasers, respectively.

#226592 - $15.00 USD Received 10 Nov 2014; revised 19 Dec 2014; accepted 20 Dec 2014; published 8 Jan 2015

Yokogawa inc. AQ6375), respectively. The core-pumped WS-laser yielded a scanning bandwidth of ~240 nm; from ~1754 nm to ~1994 nm [Fig. 3(a)]. The average output power was 420 mW for a pump power of 3.9 W. The cladding-pumped laser produced a scanning bandwidth of ~176 nm; from ~1900 nm to ~2076 nm [Fig. 3(b)]. The average output power was 360 mW for a pump power of 7.6 W. The scanning frequency was ~340 Hz corresponding to a scanning speed of ~170 μm/s for both laser configurations. In comparison with the tuning range of the aforementioned tunable lasers, the scanning bandwidths were slightly narrower in either pumping configuration. This can be attributed to the aberrations of the lenses and hence the higher insertion loss for the wavelength scanning filter. In addition, it should be noted that the spectral shapes were not continuous, but discrete. Figures 3(c)–3(f) show the temporal profiles of the core and cladding-pumped WS-lasers over 10 ms and 100 μs timescales. In both cases, it can be seen the laser output had a discrete pulsed structure and they were quite different from the temporal profiles of the WS-laser based on a semiconductor gain medium reported in [10]. The duration of each pulse was typically in the range 500 ns - 1μs, but with considerable variation in the time interval between pulses and peak power. The underlying reason for the pulsing behavior is believed to be due to the relatively long build-up time for laser emission due to the low emission cross-section for rare-earth doped glass gain media. The non-continuous spectral profile for a wavelength sweep is a direct consequence of the pulsing behavior. The spectral profiles illustrated in Figs. 3(a) and 3(b) provide a rough idea of the variation in spectral power density over a wavelength sweep for the core and cladding-pumped lasers, but it should be noted that the optical spectrum analyzer (OSA) was not synchronized with the WS-laser. Figures 4(a) and 4(b) show the maximum spectral power density as a function of wavelength at a repetition rate of 340Hz recorded over multiple scans for the core and cladding-pumped WS-lasers respectively. It can be seen that the maximum spectral power density is relatively constant for both laser configurations. The spurious peaks close to the center of the wavelength scan [Fig. 4(a)] probably correspond to parasitic lasing between the fiber end facets at wavelengths close to the gain maximum between wavelength scans (i.e. when there is no feedback from the external cavity). This represents a relatively small contribution to the overall average power and could in principal be avoided by modifying the design of the feedback arrangement and rotating prism to reduce the time interval between successive scans.

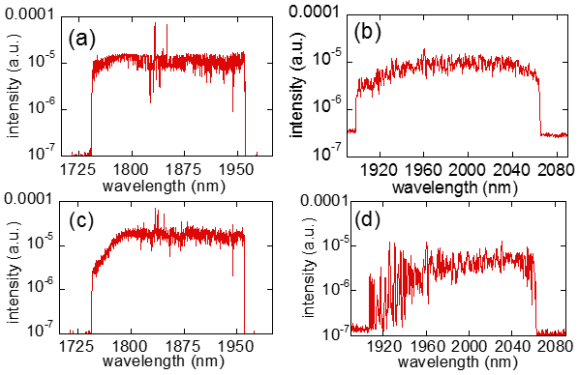

Fig. 4. Output spectra of the wavelength-swept Tm doped fiber laser measured in 'maximum-hold' mode of the OSA. (a) Core-pumped configuration at a repetition rate of ~340 Hz and (b) cladding-pumped configuration at a repetition rate of ~340 Hz. (c) Core-pumped configuration at a repetition rate of ~1 kHz and (d) cladding-pumped configuration at a repetition rate of ~1 kHz.

To investigate the influence of scanning speed on the spectrum, the WS-lasers were operated at a nearly three times higher repetition rate of 1 kHz. The resulting spectral profiles for the core and cladding-pumped laser configurations are shown in Figs. 4(c) and 4(d) respectively. The corresponding scanning speed was ~500 μm/s. In the cladding-pumped configuration, the higher scanning speed led to more pronounced pulsing behavior. In

#226592 - $15.00 USD Received 10 Nov 2014; revised 19 Dec 2014; accepted 20 Dec 2014; published 8 Jan 2015

contrast, the pulsing behavior of the core-pumped configuration was influenced far loss by the higher scanning speed. This is because of the shorter build-up time for laser emission in the core-pumped laser due to a higher single-pass gain in the fiber and shorter cavity round-trip time. The pulsing behavior could be actively suppressed by including a modulator with appropriate feedback control in both WS-lasers.

The outputs from both core and cladding-pumped WS-lasers were then spectrally combined by means of a dichroic mirror with low reflectivity (< 10%) for wavelengths >1970 nm and high reflectivity (>90%) for wavelengths <1920 nm. The dichroic mirror was designed so that the transition region (i.e. 1920-1970 nm) between high and low reflectivity coincides with the wavelength overlap region for the two WS-lasers. In this way, the wavelength could be scanned across both bands without the penalty of a significant dip in spectral power density at the centre of the combined wavelength scan. The spectrally-combined WS laser yielded over 500 mW of average output power with a scanning range from ~1740 nm to ~2070 nm for a repetition rate of ~340 Hz [see Fig. 5(a)]. In the temporal profile of the combined laser, shown in Fig. 5(b), it can clearly be seen that there are two distinct pulse envelopes corresponding to the individual lasers. The broader one corresponds to the output from the core-pumped configuration and the narrower one from the cladding-pumped configuration. These are passively synchronized by virtue of the external feedback cavities and the time interval between the outputs from the two lasers can be adjusted by changing the angle of the diffraction gratings and/or the incident angle of the laser beams on the polygon mirror. In the experiment, they were adjusted to yield a small overlap in spectral profile, but not to yield an overlap in the temporal domain.

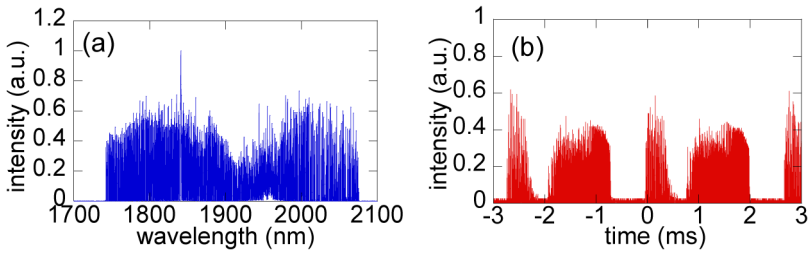

Fig. 5. (a) Spectrally-combined WS-laser output spectrum and (b) temporal profile.

4. Conclusion

In summary, we have described a wavelength-swept Tm fiber laser system employing two parallel cavities with two different fiber gain stages to achieve very wide wavelength tuning. The two fiber gain stages were tailored to have emissions in complementary bands and the two parallel cavities shared a common rotating polygon mirror for passive synchronization of their outputs. The WS-laser outputs were spectrally combined by means of a dichroic mirror and yielded over 500 mW of output and had a scanning range from 1740 nm to 2070 nm at ~340 Hz sweep rate corresponding to a wavelength sweeping speed of ~170 μm/s. This is believed to be the widest wavelength tuning range reported to date for a Tm fiber laser and, with further optimization such as shortening the gain fiber in core-pumped configuration, adapting optics to have less aberration, it should be possible to extend the scanning bandwidth to > 400 nm. This source should benefit a range of applications where broad tuning bandwidth and high spectral power density in the two-micron band are required.

Acknowledgment

Funding from UK Art and Humanities Research Council (AHRC) and Engineering and Physical Sciences Research Council (EPSRC) Science & Heritage Program (Interdisciplinary Research Grant AH/H032665/1) is gratefully acknowledged.